Journal of Kerbala University , Vol. 7 No.2 Scientific . 2009

CALCULATION OF THE INELASTIC LONGITUDINAL FORM FACTORS FOR SOME LIGHT NUCLEI

حساب عوامل التشكل للاستطارة الالكترونية الطولية
غير المرنة لبعض النوى الخفيفة

A. K. Hamoudi †, R. A. Radhi †, F.I. Shrrad Al-Taie ‡ and K. N. Flaih†
†University of Baghdad-College of Science – Department of Physics
‡University of Karbala-College of Science – Department of Physics

ABSTRACT

The inelastic longitudinal form factors *F(q)*'s, an expression for the transition charge density are studied where the deformation in nuclear collective modes is taken into consideration besides the shell model transition density. In this work, the core polarization transition density is evaluated by adopting the shape of Tassie model together with form of the ground state two-body charge density distributions and the effect of two body short range correlation function. It is noticed that the core polarization effects which represent the collective modes are essential in obtaining a good agreement between the calculated inelastic longitudinal *F(q)*'s and those of experimental data for ^{4}He, ^{12}C, ^{16}O, ^{28}Si, ^{32}S and ^{40}Ca nuclei.

الخلاصة

درست عوامل التشكل الطولية غير المرنة والمتضمنة انتقال كثافة الشحنة اخذين بالحسبان التشوه في الأنماط التجميعية النووية إلى جانب كثافة الانتقال لأنموذج القشرة. أن تأثيرات استقطاب القلب لكثافة الانتقال حسبت بالاعتماد على شكل أنموذج Tassie إلى جانب الصيغة الرياضية لتوزيعات كثافة الشحنة النووية بصيغة الجسيمين في الحالة الأرضية والمتضمنة تأثير دالة الارتباط للجسيمين. لقد وجد بان تأثير استقطاب القلب الذي يمثل نمط تجميعي يكون جوهريا للحصول على توافق جيد بين حسابات الاستطارة الطولية غير المرنة و القيم العملية لجميع النوى قيد الدراسة (^{4}He, ^{12}C, ^{16}O, ^{28}Si, ^{32}S and ^{40}Ca).

1-INTRODUCTION

Inelastic scattering of medium energy electron provides a well-understood probe of the charge, current and magnetization densities which characterized nuclear excitations. In light nuclei, where the plan-wave Born approximation is quate accurate, provided a simple correction to the momentum transfer for Coulomb distortion is made, the connection between the measured form factors and the transition densities is direct and is simply expressed as Bessel transform. Also, it is for light nuclei that the most extensive microscopic calculations of the transition densities can be performed and tested[1].

Hotta et. al. [2] measured inelastic electron scattering cross section for ^{4}He at 180º for incident electron energies of 130 and 200 MeV. Spectra, measured up to excitation energies of 54 MeV, were relatively featureless and they showed no evidence for resolvable excitations. The longitudinal and transverse form factors for ^{12}C were determined separately as a functions of the excitation energy from (15-40)MeV in the momentum transfer range (0.75-1.56) fm^{-1} by Yamaguchi et. al. [3]. The nuclear response to 200-350 MeV electron inelastically scattered at 20º for six nuclei ranging from A=9 to 181 was given. An excitation energy integral was formed and compared with theoretical calculations of the total inelastic scattering cross section [4]. The longitudinal C2 and transverse E2 form factors were analyzed in a conventional harmonic oscillator shell model. Elastic and inelastic electron scattering form factors were calculated for the similar parity states of 1p-shell nuclei in the frame work of the many particles shell model including core-polarization effects by Adeeb [5].

Inelastic electron scattering with high energy resolution was used by Miska et. al. [6] to study the states at 6.05 (0^{+}), 6.13 (3^{-}) and 6.92 (2^{+}) MeV excitation energy in ^{16}O for momentum transfers q = 0.22 – 0.49 fm^{-1}.

Coulomb form factors of C4 transitions in even-even N = Z sd-shell nuclei (^{20}Ne, ^{24}Mg, ^{28}Si and ^{32}S) have been discussed by Radhi [7] taking into account higher-energy configurations outside the sd-shell model space which are called core polarization effects. Higher configurations are taken into account through a microscopic theory, which allows particle-hole excitations from the 1s and 1p shells core orbits and also from the 2s1d-shell orbits to the higher allowed orbits with excitations up to $4\hbar\omega$. The effect of core polarization was found essential in both the transition strengths and momentum transfer dependence of form factors, and gives a remarkably good agreement with the measured data with no adjustable parameters. The calculations were based on the Wildenthal interaction for the sd-shell model space and on the modified surface delta interaction (MSDI)for the core polarization effects. Shell-model wave functions obtained from a unified treatment of the structure of the positive parity states in sd- shell nuclei have been used by Flaih [8] to calculate the feature of the inelastic transition from J^{π} ($0^+ \rightarrow 2^+$ and 4^+) states in this region. Inelastic electron scattering to 2^+ and 4^+ states for the even-even N=Z sd-shell nuclei have been discussed by Radhi and Boucheback [9] and Boucheback [10] taking into account core-polarization effects. These effects were included through a microscopic theory that includes excitation from the core 1s and 1p orbits and also from 2s-1d shell to the higher allowed orbits with $2\hbar\omega$ excitation. These effects were found essential in both the transition strength and momentum transfer dependence of form factors and they gave remarkably good agreement with the data.

The purpose of the present work are to calculate the longitudinal C0, C2 and C4 form factors for the inelastic electron scattering ^{4}He, ^{12}C, ^{16}O, ^{28}Si, ^{32}S *and* ^{40}Ca nuclei depending on the ground state two body charge density distributions which included the effect of two body short range correlation. The Cohen-Kurath (CK) and Wildenthal (W)interactions are used to get the p- and sd-shell model space wave functions, respectivly. The results will be compared with the available experimental data and for different range of momentum transfer q.

2-THEORY

2-1 Inelastic Longitudinal Form Factors

Inelastic longitudinal electron scattering form factors involving angular momentum J and momentum transfer q which can be written as [11].

$$\left|F_J^L(q)\right|^2 = \frac{4\pi}{Z^2(2J_i+1)}\left|\left\langle f\left\|\hat{T}_J^L(q)\right\|i\right\rangle\right|^2 \left|F_{cm}(q)\right|^2 \left|F_{fs}(q)\right|^2 \qquad (1)$$

where $\hat{T}_J^L(q)$ is the longitudinal electron scattering operator, $F_{fs}(q)$ is the finite nucleon size correction, $F_{cm}(q)$ is the center of mass correction and Z is the atomic number. The nuclear states have well defined isospin $T_{i/f}$, therefore the form factors of eq (1) may be written in terms of the matrix elements reduced in both angular momentum and isospin [12].

$$\left|F_J^L(q)\right|^2 = \frac{4\pi}{Z^2(2J_i+1)}\left|\sum_{T=0,1}(-1)^{T_f-T_{zf}}\begin{pmatrix} T_f & T & T_i \\ -T_{Z_f} & 0 & T_{Z_i}\end{pmatrix}\left\langle f\left\|\hat{T}_{JT}^L(q)\right\|i\right\rangle\right|^2$$
$$\left|F_{cm}(q)\right|^2 \left|F_{fs}(q)\right|^2 \qquad (2)$$

where T is restricted by the following selection rule:

$$\left|T_f - T_i\right| \le T \le T_f + T_i \qquad (3)$$

and $T_Z = \frac{Z-N}{2}$. The bracket $(\quad)$ in eq (2) is the three $-j$ symbol and the reduced matrix elements in spin and isospin space of the longitudinal operator between the final and initial many particles states of the system including the configuration mixing are given in terms of the One Body

Density Matrix (OBDM) elements times the single particle matrix elements of the longitudinal operator[13], i.e.

$$\left\langle f \left\| \hat{T}^{L}_{JT} \right\| i \right\rangle = \sum_{a,b} OBDM^{\,JT}(i,f,J,a,b) \left\langle b \left\| \hat{T}^{L}_{JT} \right\| a \right\rangle \qquad (4)$$

The OBDM elements are calculated in terms of the isospin–reduced matrix elements [14], i.e.

$$OBDM(\tau_Z) = (-1)^{T_f - T_z} \begin{pmatrix} T_f & 0 & T_i \\ -T_Z & 0 & T_Z \end{pmatrix} \sqrt{2}\ \frac{OBDM\,(\Delta\ T = 0)}{2}$$

$$+\tau_Z (-1)^{T_f - T_z} \begin{pmatrix} T_f & 1 & T_i \\ -T_Z & 0 & T_Z \end{pmatrix} \sqrt{6}\,\frac{OBDM(\Delta T = 1)}{2} \qquad (5)$$

The OBDM(ΔT) is defined [14] as :

$$OBDM\,(i,f,j,j',\Delta T) = \frac{\left\langle f \left\| \left[a^{+}_{j} \times \tilde{a}_{j'}\right]^{J,\Delta T} \right\| i \right\rangle}{\sqrt{2J+1}\ \sqrt{2\Delta T+1}} \qquad (6)$$

The operator a^{+}_{j} creates a neutron or proton in the single nucleon state j and the operator $\tilde{a}_{j'}$ annihilates a neutron or proton in the single nucleon state j'.

2-2 Core – Polarization Effects

The model space matrix elements is not adequate to describe the absolute strength of the observed gamma-ray transition probabilities, because of the polarization in nature of the core protons by the model space protons and neutrons [15]. Therefore the many particle reduced matrix elements of the longitudinal operator, consists of two parts one is for the model space and the other is for core polarization matrix element [16].

$$\left\langle f \left\| \hat{T}^{L}_{J}(\tau_Z,q) \right\| i \right\rangle = \left\langle f \left\| \overset{ms}{\hat{T}^{L}_{J}}(\tau_Z,q) \right\| i \right\rangle + \left\langle f \left\| \overset{core}{\hat{T}^{L}_{J}}(\tau_Z,q) \right\| i \right\rangle \qquad (7)$$

where the model space matrix element in eq.(7) has the form [16].

$$\left\langle f \left\| \overset{ms}{\hat{T}^{L}_{J}}(\tau_Z,q) \right\| i \right\rangle = e_i \int_0^\infty d\mathrm{r}\,\mathrm{r}^2 j_J(q\mathrm{r}) \overset{ms}{\rho}_{J,\tau_Z}(i,f,\mathrm{r}) \qquad (8)$$

The model space transition density $\overset{ms}{\rho}_{J,\tau_Z}(i,f,\mathrm{r})$ is expressed as the sum of the product of the OBDM times the single particle matrix elements, and is given by [14].

$$\overset{ms}{\rho}_{J,\tau_Z}(i,f,\mathrm{r}) = \sum_{jj'(ms)}^{ms} OBDM(i,f,J,j,j',\tau_z) \left\langle j \| \mathrm{Y}_J \| j' \right\rangle R_{nl}(\mathrm{r})\ R_{n'l'}(\mathrm{r}) \qquad (9)$$

where $R_{nl}(\mathrm{r})$ is the radial part of the harmonic oscillator wave function .

The core- polarization matrix element in eq. (7) takes the following form [16].

$$\left\langle f \left\| \overset{core}{\hat{T}^{L}_{J}}(\tau_Z,q) \right\| i \right\rangle = e_i \int_0^\infty d\mathrm{r}\,\mathrm{r}^2 j_J(q\mathrm{r}) \overset{core}{\rho}_{J}(i,f,\mathrm{r}) \qquad (10)$$

where $\overset{core}{\rho}_{J}$ is the Core- Polarization transition density which depends on the model used for core polarization. To take the core- polarization effects into consideration, the model space transition density is added to the core-polarization transition density that describes the collective modes of nuclei. The total transition density becomes

$$\rho_{J\tau_Z}(i,f,\mathrm{r}) = \overset{ms}{\rho}_{J\tau_Z}(i,f,\mathrm{r}) + \overset{core}{\rho}_{J\tau_Z}(i,f,\mathrm{r}) \qquad (11)$$

In the present work, the shape of the Tassie Model (TM) is employed for core-polarization.

2-3 Tassie – Model

This model has been used to describe gamma-transition and the excitation of nuclei by electron scattering. It is the multiple analysis of the inelastic scattering. For a uniform charge distribution this model is reduced to the usual liquid drop model. Tassie–Model is an attempt to a model with more elasticity and modification that permits for a non-uniform charge and mass density distribution. According to this model, the core- polarization transition density depends on the ground state charge density of the nucleus. In this work, the ground state charge density is formulated in terms of the two-body charge density for all occupied shells including the core. According to the collective modes of nuclei, the core polarization transition density is given by the Tassie shape [17].

$$\rho_{Jt_z}^{core}(i,f,\mathrm{r}) = N\frac{1}{2}(1+\tau_z)\,\mathrm{r}^{J-1}\frac{d\rho_o(i,f,\mathrm{r})}{d\mathrm{r}} \qquad (12)$$

where N is a proportionality constant and ρ_o is the ground state two – body charge density distribution, which is given

$$\rho_o = \langle \Psi \mid \hat{\rho}_{eff}^{(2)}(\vec{\mathrm{r}}) \mid \Psi \rangle = \sum_{i\langle j}\langle i\ j|\ \hat{\rho}_{eff}^{(2)}(\vec{\mathrm{r}})\ \left[\,|\ ij\ \rangle - |\ ji\ \rangle\,\right] \qquad (13)$$

where [18]: $$\hat{\rho}_{eff}^{(2)}(\vec{\mathrm{r}}) = \frac{1}{2(A-1)}\ f(r_{ij})\sum_{\mathrm{i}\neq\mathrm{j}}\left\{\delta(\vec{\mathrm{r}}-\vec{\mathrm{r}}_{\mathrm{i}}) + \delta(\vec{\mathrm{r}}-\vec{\mathrm{r}}_{\mathrm{j}})\right\} f(r_{ij}) \qquad (14)$$

and i and j are all the required quantum numbers, i.e.

$i \equiv n_i, \ell_i, j_i, m_i, t_i, m_{t_i}$ and $j \equiv n_j, \ell_j, j_j, m_j, t_j, m_{t_j}$

where the functions $f(\mathrm{r}_{\mathrm{ij}})$ are the two – body short range correlation (SRC). In this work, a simple model form of short range correlation of Ref. [18] will be adopted, i.e.

$f(\mathrm{r}_{\mathrm{ij}}) = 1 - \exp[-\beta(\mathrm{r}_{\mathrm{ij}} - \mathrm{r}_{\mathrm{c}})^2\ ]$

where r_{c} is the radius of a suitable hard – core and β is a correlation parameter.

The Coulomb form factor for this model becomes:-

$$F_J^L(q) = \sqrt{\frac{4\pi}{2J_i+1}}\,\frac{1}{Z}\left\{\int_0^\infty \mathrm{r}^2 j_J(q\mathrm{r})\,\rho_J^{ms}(i,f,\mathrm{r})\,d\mathrm{r}\right.$$
$$\left. + N\int_0^\infty d\mathrm{r}\,\mathrm{r}^2 j_J(q\mathrm{r})\,\mathrm{r}^{J-1}\,\frac{d\rho_o(i,f,\mathrm{r})}{d\mathrm{r}}\right\} F_{cm}(q)\,F_{fs}(q) \qquad (15)$$

The radial integral $\int_0^\infty d\mathrm{r}\ \mathrm{r}^{J+1} j_J(q\mathrm{r})\frac{d\rho_o(i,f,\mathrm{r})}{d\mathrm{r}}$ can be written as:-

$$\int_0^\infty \frac{d}{d\mathrm{r}}\left\{\mathrm{r}^{J+1}\ j_J(q\mathrm{r})\,\rho_o(i,f,\mathrm{r})\right\}d\mathrm{r} - \int_0^\infty d\mathrm{r}\ (J+1)\,\mathrm{r}^J\ j_J(q\mathrm{r})\,\rho_o(i,f,\mathrm{r})$$
$$-\int_0^\infty d\mathrm{r}\ \mathrm{r}^{J+1}\frac{d}{d\mathrm{r}}\,j_J(q\mathrm{r})\,\rho_o(i,f,\mathrm{r}) \qquad (16)$$

where the first term gives zero contribution, the second and the third term can be combined together as

$$-q\int_0^\infty d\mathrm{r}\,\mathrm{r}^{J+1}\rho_o(i,f,\mathrm{r})\left[\frac{d}{d(q\mathrm{r})} + \frac{J+1}{q\mathrm{r}}\right] j_J(q\mathrm{r}) \qquad (17)$$

From the recursion relation of spherical Bessel function:

$$\left[\frac{d}{d(q\mathrm{r})}+\frac{J+1}{q\mathrm{r}}\right] j_J(q\mathrm{r}) = j_{J-1}(q\mathrm{r}) \qquad (18)$$

$$\therefore \int_0^\infty d\mathrm{r}\, \mathrm{r}^{J+1} j_J(q\mathrm{r}) \frac{d\rho_o(i,f,\mathrm{r})}{d\mathrm{r}} = -q\int_0^\infty d\mathrm{r}\, \mathrm{r}^{J+1} j_{J-1} \rho_o(i,f,\mathrm{r}) \qquad (19)$$

Therefore, the form factor of eq. (15) takes the form:

$$F_J^L(q) = \left(\frac{4\pi}{2J_i+1}\right)^{1/2} \frac{1}{Z}\left\{\int_0^\infty \mathrm{r}^2 j_J(q\mathrm{r}) \overset{ms}{\rho}_{Jt_z}\, d\mathrm{r} - Nq\int_0^\infty d\mathrm{r}\,\mathrm{r}^{J+1}\rho_o\, j_{J-1}(q\mathrm{r})\right\}$$
$$\times F_{cm}(q) F_{fs}(q) \qquad (20)$$

The proportionality constant *N* can be determined from the form factor evaluated at *q=k*, i.e. substituting *q=k* in eq. (20), we obtain

$$N = \frac{\int_0^\infty d\mathrm{r}\,\mathrm{r}^2 j_J(k\mathrm{r}) \rho_{Jt_Z}^{ms}(i,f,\mathrm{r}) - F_J^L(k) Z\sqrt{\frac{2J_i+1}{4\pi}}}{k\int_0^\infty d\mathrm{r}\,\mathrm{r}^{J+1}\rho_o(i,f,\mathrm{r})\, j_{J-1}(k\mathrm{r})} \qquad (21)$$

The reduced transition probability $B(CJ)$ is written in terms of the form factor in the limit $q=k$ (photon point) as [13].

$$B(CJ) = \frac{[(2J+1)!!]^2 Z^2 e^2}{4\pi k^{2J}} \left| F_J^L(k)\right|^2 \qquad (22)$$

In eq(22), the form factor at the photon point *q=k* is related to the transition strength *B(CJ)*. Thus using eq(22) in eq(21) leads to give

$$N = \frac{\int_0^\infty dr\, r^2 j_J(kr) \rho_{Jt_z}^{ms}(i,f,r) - \sqrt{\frac{(2J_i+1)B(CJ)}{[(2J+1)!!]^2}}\, k^J}{k\int_0^\infty dr\, r^{J+1}\rho_o(i,f,r)\, j_{J-1}(kr)} \qquad (23)$$

where [13]:

$$\left.\begin{aligned} j_j(k\mathrm{r}) &= \frac{(k\mathrm{r})^J}{(2J+1)!!} \\ J_{J-1}(k\mathrm{r}) &= \frac{(k\mathrm{r})^{J-1}}{(2J-1)!!} \end{aligned}\right\} \qquad (24)$$

Introducing eq.(24) into eq.(23) , we obtain:

$$N = \frac{\int_0^\infty d\mathrm{r}\,\mathrm{r}^{J+2}\rho_{Jt_Z}^{ms}(i,f,\mathrm{r}) - \sqrt{(2J_i+1)B(CJ)}}{(2J+1)\int_0^\infty d\mathrm{r}\,\mathrm{r}^{2J}\rho_o(i,f,\mathrm{r})} \qquad (25)$$

The proportionality constant *N* can be determined by adjusting the reduced transition probability *B(CJ)* using eq. (25) with the experimental value of *B(CJ).*

3-RESULTS, DISCUSSIONS AND CONCLUSIONS

The inelastic longitudinal electron scattering form factors are calculated using the expression for the transition charge density. The model space transition density is obtained using eq. (9), where the OBDM elements are taken from the interaction matrix elements of Cohen-Kurath (CK) [19] and Wildenthal (W) [20] for 1p-shell and 2s-1d shell nuclei, respectively. For considering the collective modes of the nuclei, the core polarization transition density of eq.(12) is evaluated by adopting the Tassie model [21] together with the ground state two body charge density distributions of equation (13).

In figures (1) to (8), the calculated results for inelastic longitudinal form factors of all nuclei under study are plotted versus the momentum transfer q and compared with those of experimental results for the transitions $\left(J_i^{\pi} T_i \rightarrow J_f^{\pi} T_f\right)$. It is important to point out that all transitions considered in the present work are of an isoscalar character. In addition, the parity of these transitions does not change. Let us first explore the calculated results for some light closed shell ^{4}He , ^{16}O , and ^{40}Ca nuclei. Where these nuclei are cores of closed shell only, i.e. there are no valence (active) particles moving outside these cores. Therefore, these nuclei have no model space contribution, i.e. the longitudinal form factors of these nuclei comes totally from the core polarization only. Figure (1) shows the inelastic longitudinal C0 form factors for the transition $0_1^+ \, 0 \rightarrow 0_2^+ \, 0$ in ^{4}He nucleus. In this transition, the electron excites the nucleus from the ground state $0_1^+ \, 0$ to the excited state $0_2^+ \, 0$ with an excitation energy of E_x= 27.17 MeV. The experimental reduced transition probability B(C0) is equal to 2.02±0.32 $e^2.fm^2$ [22]. The dashed and solid curves are the calculated core polarization form factors without and with the inclusion of the effect of the two body short range correlation functions(SRC) while the dotted symbols are those of experimental data taken from Ref. [22]. It is obvious from this figure that the calculated C0 form factors (the dashed and solid curves) predict the data clearly throughout the whole range of momentum transfer q. The inelastic longitudinal C2 form factors for the transition $0_1^+ \, 0 \rightarrow 2_1^+ \, 0$ in ^{16}O nucleus is presented in figure (2). Here, the nucleus is excited from the ground state $0_1^+ \, 0$ to the state $2_1^+ \, 0$ with an excitation energy of E_x= 6.917 MeV. The experimental reduced transition probability B(C2) is equal to 40±10.8 e^2. fm^4 [23]. The C2 form factors of ^{16}O nucleus without and with the effect of SRC's (the dashed and solid curves, respectively) are in a satisfactory description with the experimental data [24].It is clear that the magnitude of the C2 form factor along the first and second maximum are very well reproduced. Furthermore, the measured diffraction minimum is reproduced at the correct momentum transfer. In figure (3) we present the inelastic longitudinal C2 form factors for the transition $0_1^+ \, 0 \rightarrow 2_1^+ \, 0$ in ^{40}Ca nucleus. In this transition the nucleus is excited by the electron from the ground state $0_1^+ \, 0$ to the excited state $2_1^+ \, 0$ with an excitation energy of E_x= 2.0 MeV. The experimental reduced transition probability B(C2) is equal to 84±3.0 $e^2.fm^4$ [25]. The dashed and solid curves are the C2 form factors of ^{40}Ca nucleus without and with the effect of SRC's, respectively whereas the dotted and triangle symbols are those of measured data of Ref's [25] and [22], respectively. The available data of this transition are restricted for a small region of momentum transfer ($q < 1.4$ fm^{-1}). In the first maximum, a best coincidence for the form factors is obtained between the calculation (the dashed and solid curves) and the experimental data, i.e. the calculated form factors are in a very good agreement with the experimental data up to momentum transfer region of $q \leq 1$ fm^{-1}. While for $1 \leq q \leq 1.4$ fm^{-1}, the data is underestimated by the calculated results. However, the behavior of the calculated C2 form factors agrees quite well with the experimental data. In addition, the calculated results for the C2 form factors reproduce the diffraction minimum at the correct momentum transfer. The inelastic longitudinal C2 form factors of ^{12}C, ^{28}Si and ^{32}S open shell nuclei are presented in figures (4), (5) and (6), respectively. Here, the calculated longitudinal C2 form factors are plotted as function of the momentum transfer (q) for the transitions, $\left(J_i^{\pi}\, T_i \rightarrow J_f^{\pi}\, T_f\right), 0^+ 0 \rightarrow 2_1^+ 0$ (E$_x$=4.44 MeV, B(C2)= 38.81±2.15 e^2.fm^4 [26]) in ^{12}C , $0^+ 0 \rightarrow 2_1^+ 0$ (E$_x$ =1.78 MeV, B(C2)= 327.24±9.47 e^2.fm^4[20]) in ^{28}Si and $0^+ 0 \rightarrow 2_1^+ 0$ (E$_x$ =2.237 MeV,B(C2)=300.33±11.9 e^2.fm^4[20]) in ^{32}S. In these figures, the dash- dotted curves represent the contribution of the model space where the configuration mixing is taken into account, the dashed curves represent the core polarization contribution where the effect of SRC's is considered, the solid curves represent the total contribution, which is obtained by taking the model space together with the core polarization effects into consideration and the dotted symbols represent the experimental data of ^{12}C [27], ^{28}Si[28] and ^{32}S [29]. The OBDM elements for the above transitions are given in tables (1), (2) and (3) for ^{12}C, ^{28}Si and ^{32}S nuclei, respectively . These figures show that the contribution of the model space can not reproduce the experimental data since it underestimates the data for all values of momentum transfer. Considering the effect of core polarization together with the model space (the solid curves), leads to give an enhancement to the longitudinal C2 form factors and consequently to make the calculated results to be in a satisfactory description with those of the experimental data for all values of momentum transfer q . The inelastic longitudinal C4 form factors for ^{28}Si are displayed in figure (7). Here, the electron excites the ^{28}Si nucleus from the ground state $(J_i^{\pi}T_i = 0_1^+0)$ to the excited state $(J_f^{\pi}T_f = 4_1^+0)$ with excitation energy of 4.617 MeV. The experimental reduced transition probability B(C4) is equal to 27.5±5.0×10^3 e^2.fm^8 [20]. The values of the one-body density matrix elements (OBDM) for this transition are illustrated in table (4).In this figure, the contribution of the model space is represented by the dash- dotted curve, the core polarization contribution with the effect of the SRC's is represented by the dashed curve and the total contribution is represented by the solid curve and obtained by taking the model space together with the core polarization effects into consideration. This figure shows that the model space is not able to give a satisfactory description with the experimental data for the region of momentum transfer $q <$ 2 fm^{-1} but once the core polarization effect is added to the model space, the obtained results for the longitudinal C4 form factors become in a good agreement with the experimental data throughout the whole range of momentum transfer q. In figure (8), we present the form factors for the combination of the first $J_f^{\pi}T_f = 4_1^+0$ state (with excitation energy 4.46 MeV and B(C4)= 49.9 e^2.fm^8 [30]) and the second $J_f^{\pi}T_f = 2_2^+0$ state (with excitation energy 4.482 MeV and B(C2)= 6.65±0.48 e^2.fm^4 [20]) of ^{32}S nucleus. The one-body density matrix elements for these transitions are shown in table (5) and table (6). In fact, many attempts were made to explain the C4 transition in the upper half of the 2s-1d shell nuclei for the mass region $(30 \leq A \leq 40)$. In this region, there is no available data for the C4 electron scattering that can be used in the analysis. The most logical candidate for improving this situation would seem to be the ^{32}S nucleus, where an extensive C2 results are available. The main difficulty that prevents the calculations to be improved with the ^{32}S nucleus is concerned with the closeness of the first $4^+{}_1 0$ and the second $2^+{}_2$ states in which their experimental energy separation is quite small and it turns out to prevent the experiments of electron scattering of resolving them. However, the calculated form factors of ^{32}S doublet is presented in figure (8). The dash – dotted curve represents the total C2 form factors which includes both contributions of the model space and core polarization effect, the dashed curve represents the total C4 form factors with both contributions as well, the solid curve represents the sum of C2 and C4 contributions and the dotted symbols represent the experimental form factors taken from Ref.[31]. As we can see from this figure that beyond 1.4fm^{-1} ($q >$ 1.4 fm^{-1}), the form factor is predicted to be nearly totally from C4 excitation .In general, the comparison between the experimental data and the combined $(2^+{}_2)$ and $(4^+{}_1 0)$ calculated form factors is in excellent agreement since the solid curve shows a nicely consistency with the available data.

Figures (1) to (3) give the conclusion that the effect of the inclusion of the two body SRC's is small in the calculations of the inelastic longitudinal form factors of closed shell nuclei and even it becomes gradually smaller with increasing the mass number A of closed shell nuclei. Figures (4) to (8) give the conclusion that the core polarization effects which represent the collective modes are essential in obtaining a remarkable agreement between the calculated inelastic longitudinal *F(q)*'s and those of experimental data for all considered nuclei.

Table (1): The values of the OBDM elements for the longitudinal C2 form factors of the isoscalar transition ($2^+ 0$) at E_x = 4.44 MeV for ^{12}C [19].

$2j_i$	$2j_f$	$OBDM$ (ΔT =0)
3	3	0.0000000
3	2	0.7591841
2	3	-0.5011840
2	2	-0.3097547

Table (2): The values of the OBDM elements for the longitudinal C2 form factors of the isoscalar transition ($2^+ 0$) at E_x =1.78 MeV for ^{28}Si [20]

$2j_i$	$2j_f$	$OBDM$ (ΔT =0)
5	5	-0.2986
5	1	-0.4066
5	3	-0.3038
1	5	-0.5949
1	3	-0.0862
3	5	0.3835
3	1	0.1532
3	3	-0.1714

Table (3): The values of the OBDM elements for the longitudinal C2 form factors of the isoscalar transition ($2^+ 0$) at E_x = 2.237 MeV for ^{32}S [20]

$2j_i$	$2j_f$	$OBDM$ (ΔT =0)
5	5	-0.0701
5	1	-0.1542
5	3	-0.1105
1	5	-0.2155
1	3	-0.3730
3	5	0.1178
3	1	0.6000
3	3	-0.2492

Table (4): The values of the OBDM elements for the longitudinal C4 form factors of the isoscalar transition (4^+ 0) at E_x = 4.617 MeV for ^{28}Si [20].

$2j_i$	$2j_f$	*OBDM* (ΔT =0)
5	5	-0.0032
5	3	-0.2413
3	5	0.4981

Table (5): The values of the OBDM elements for the longitudinal C2 form factors of the isoscalar transition (2_2^+ 0) at E_x = 4.282 MeV for ^{32}S [20].

$2j_i$	$2j_f$	*OBDM* (ΔT =0)
5	5	0.0906
5	1	0.1547
5	3	0.1557
1	5	0.2620
1	3	0.0456
3	5	-0.4069
3	1	-0.0516
3	3	-0.1443

Table (6): The values of the OBDM elements for the longitudinal C4 form factors of the isoscalar transition (4^+ 0) at E_x = 4.46 MeV for ^{32}S [20].

$2j_i$	$2j_f$	*OBDM* (ΔT =0)
5	5	-0.0819
5	3	-0.2690
3	5	0.5603

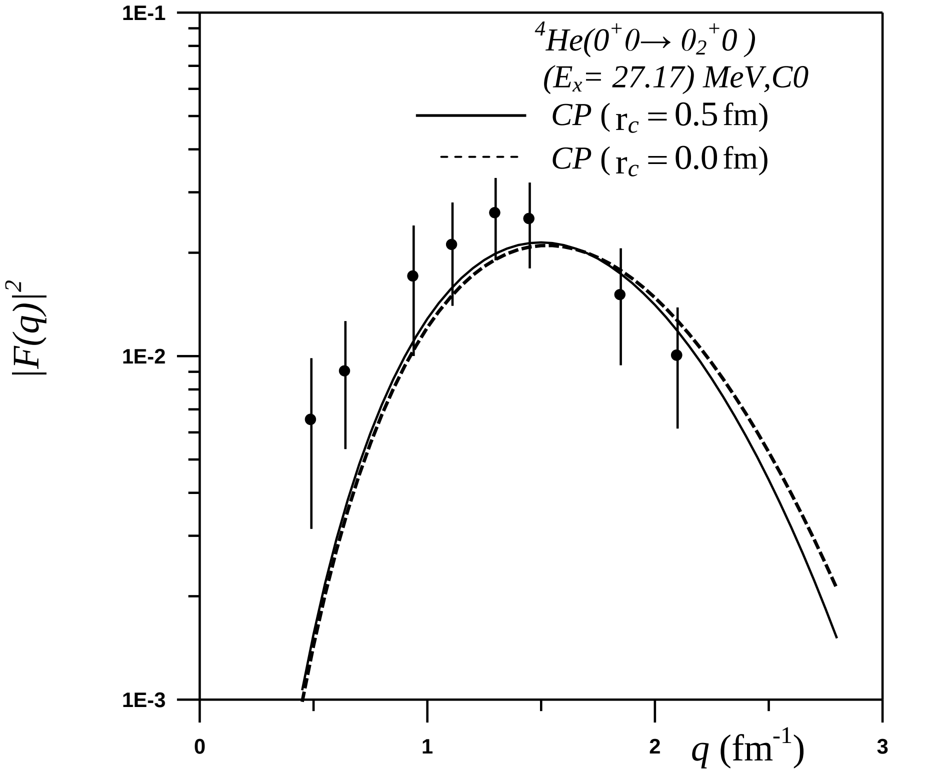

Figure (1): Inelastic longitudinal C0 form factors for ^{4}He nucleus.
The dotted symbols are the experimental data of Ref [22].

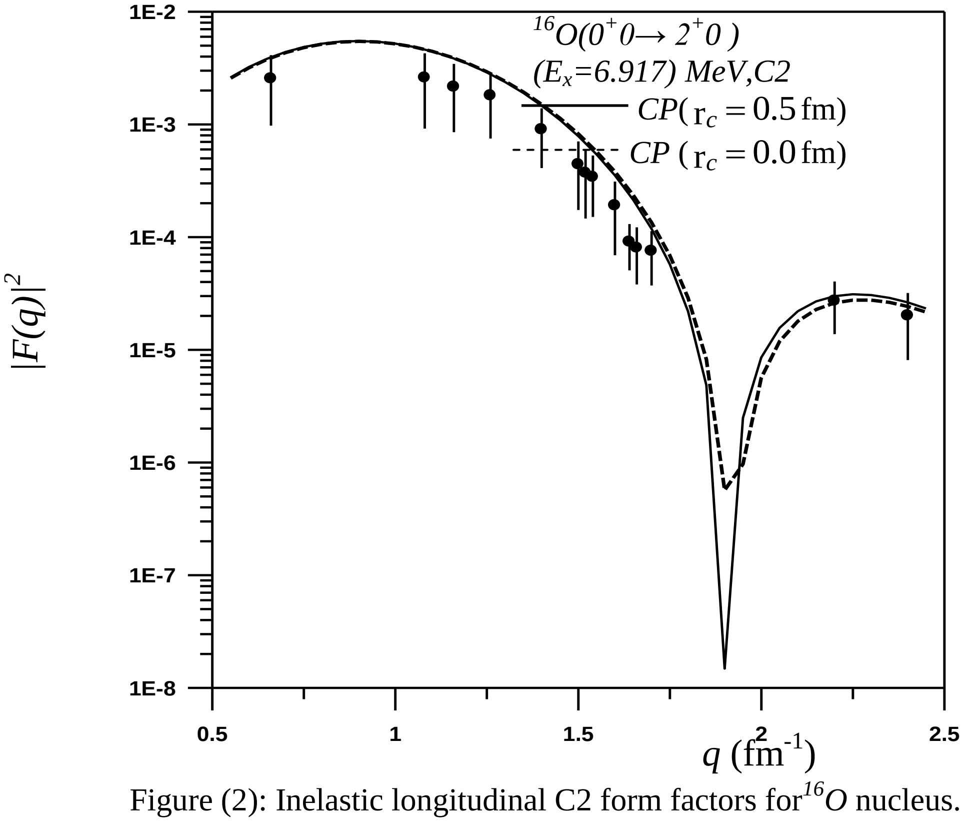

Figure (2): Inelastic longitudinal C2 form factors for ^{16}O nucleus.
The dotted symbols are the experimental data of Ref. [24].

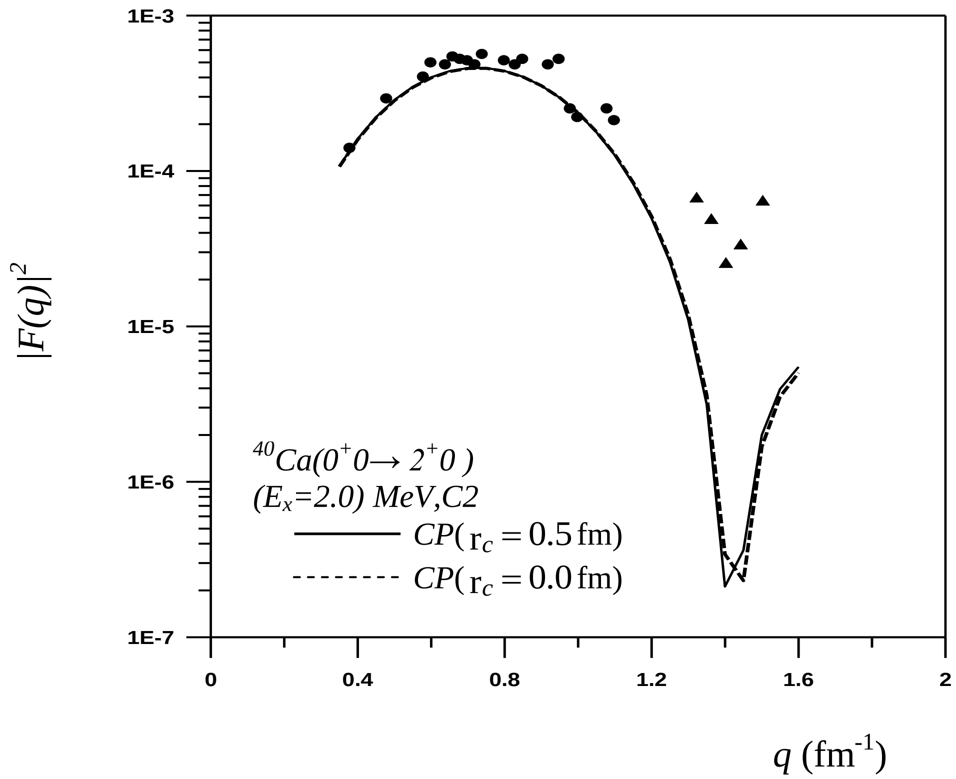

Figure (3): Inelastic longitudinal C2 form factors for ${}^{40}Ca$ nucleus. The dotted and triangle symbols are the experimental data of Ref's. [25] and [22] respectively.

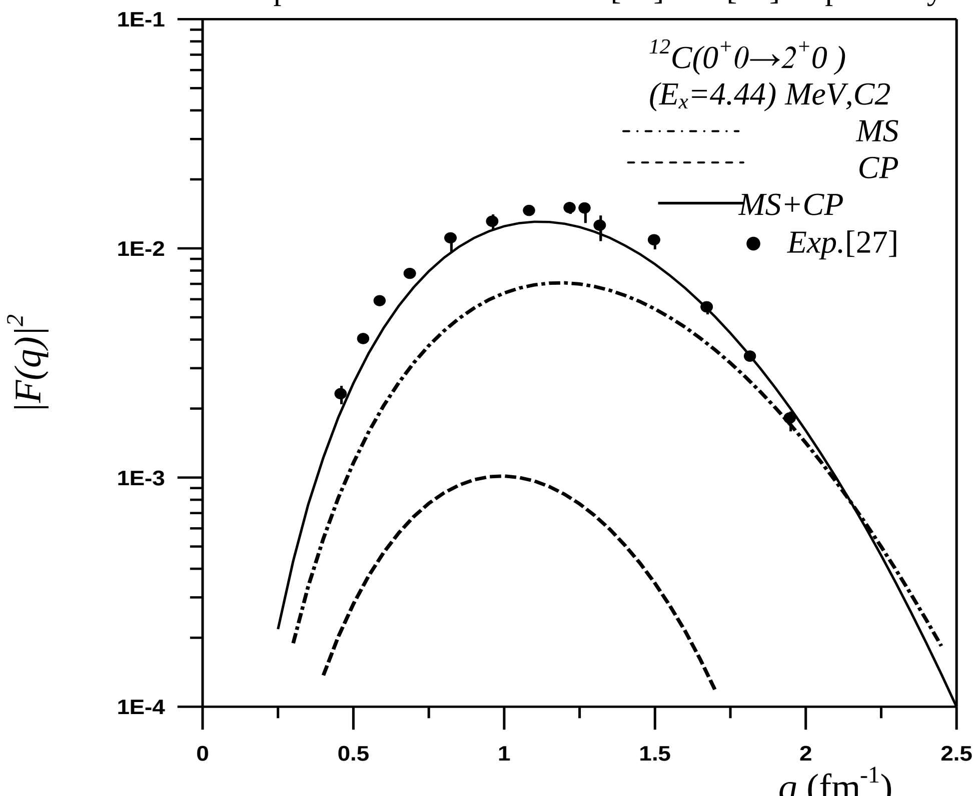

Figure (4):Inelastic longitudinal C2 form factors for ${}^{12}C$ nucleus.

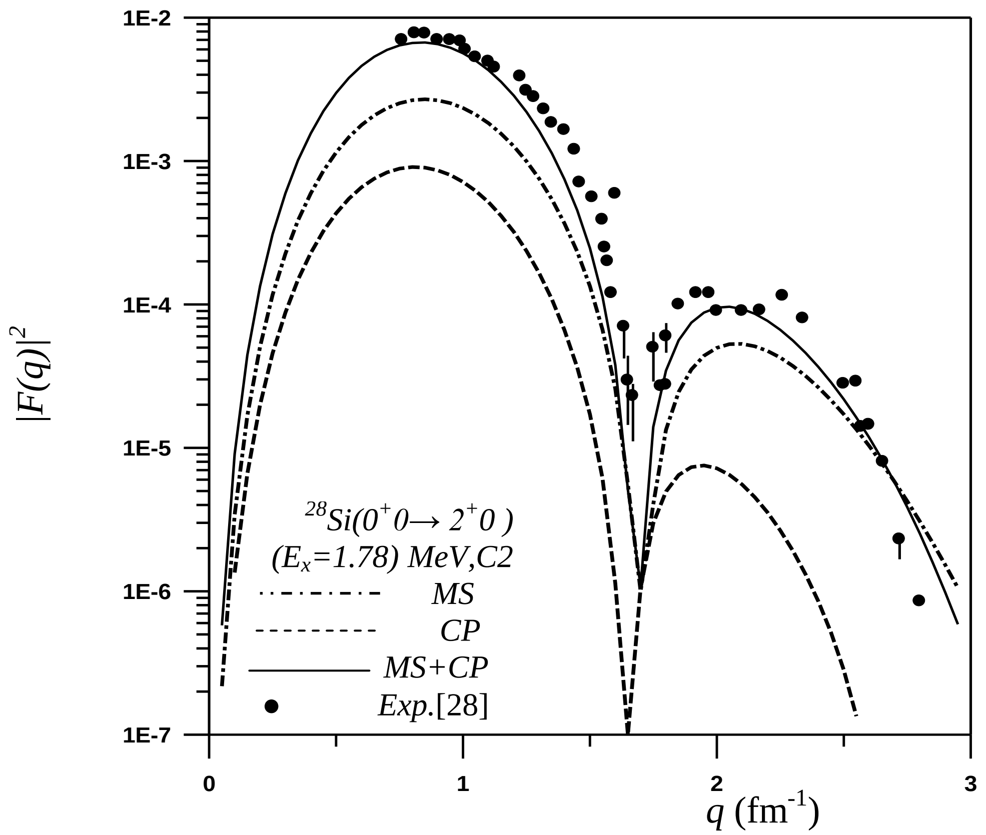

Figure (5):Inelastic longitudinal C2 form factors for ^{28}Si nucleus.

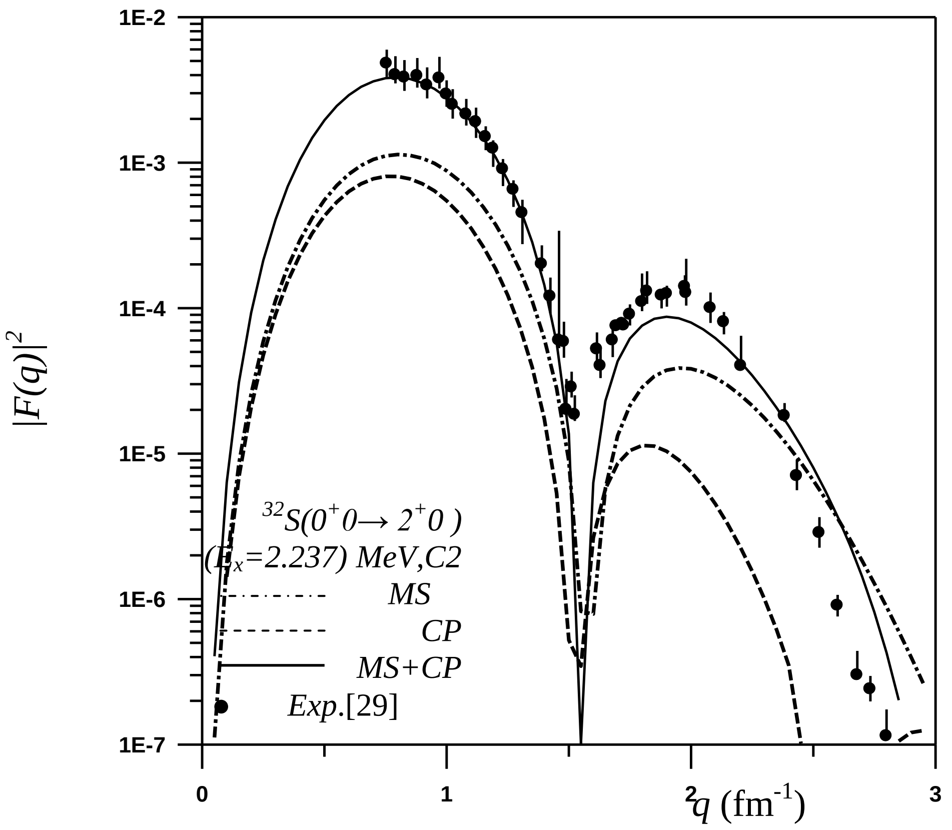

Figure (6):Inelastic longitudinal C2 form factors for ^{32}S nucleus.

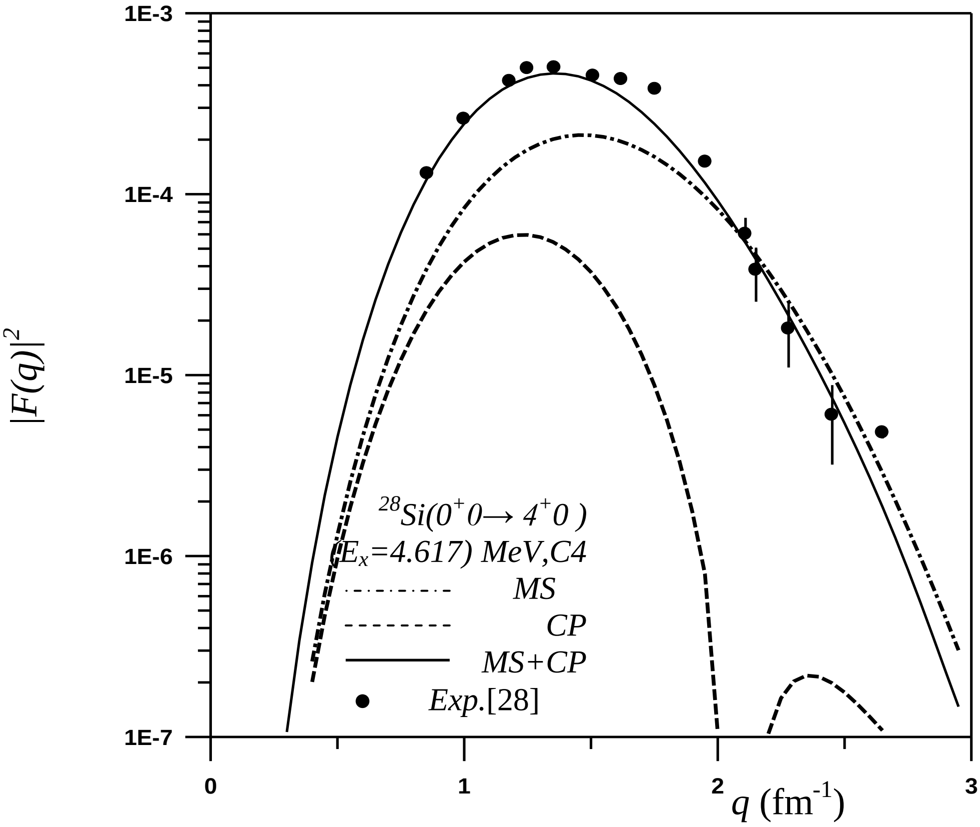

Figure (7): Inelastic longitudinal C4 form factors for ^{28}Si nucleus.

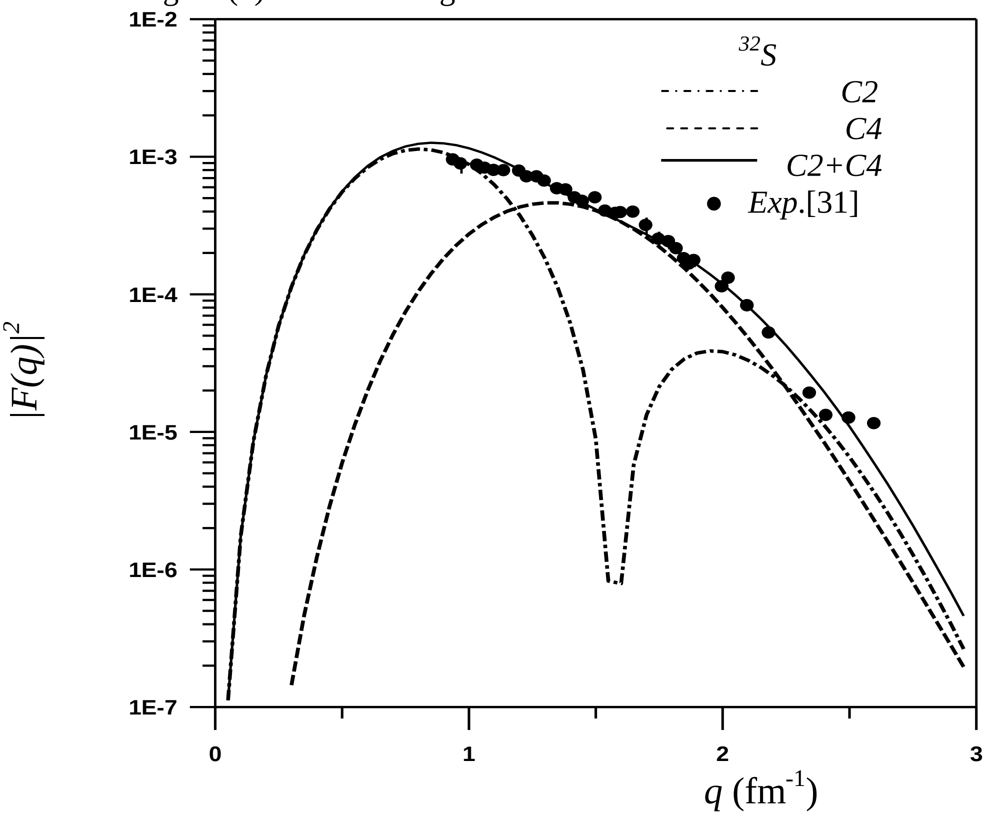

Figure (8): Experimental and Theoretical form factors for the 4.282 MeV 2_2^+ + 4.46 MeV 4_1^+ doublet in ^{32}S.

REFERENCES

[1]D. J. Millener, D. J. Sober, H. Crannell, J. T. O'Brien, L. W. Fagg, S. Kowalski, C. F. Williamson and L. Lapikas, Phys. Rev., C39, 39 , (1989) .
[2]A. Hotta, J. Dubach, R. S.Hicks, R. L. Huffmann, B. Parker, G. A. Peterson, P. J. Ryan, R. P. Singhal and D. Halderson; Phys. Rev., C38, 1547, (1988).
[3]A.Yamaguchi,T.Terasawa,K.Nakahara and Y.Torizuka;Phys.Rev., C3, 1750, (1971).
[4]J.S.O'Connell,E.Hayward,J.W.Lightbody,X.K.Maruyama,P.Bosted, K. I. Blomquist, G.Franklin, J-O.Adler, K.Hansen and B.Schroder; Phys. Rev., C27, 2492, (1983).
[5]N.Adeeb; Ph.D.thesis, College of Science, University of Baghdad, (2001).
[6]H.Miska, H.D.Graf, A.Richter, R.Schneider, D.Schull, E.Spamer, H.Theissen, O.Titze, Th.Walcher; Phys. Lett., 58B, 155, (1975).
[7]R.A.Radhi ; Eur. Phys. J., A16, 381, (2003).
[8]K.Flaih;M.Sc.thesis, College of Science, University of Baghdad, (2003).
[9]R.A.Radhi and A.Boucheback ; Nucl. Phys., A716,87,(2003).
[10]A. Bouchebak; M. Sc. thesis, College of Science, University of Baghdad, (2003).
[11]B. A. Brown, B. H. Wildenthal, C. F. Williamson, F. N. Rad, S. Kowalski, H. Crannell and J. T. O'Brien, Phys. Rev., C32, 1127, (1985).
[12]T. W. Donnelly and I. Sick, Rev. Mod. Phys., 56, 461, (1984).
[13]P.J.Brussard and P.W.M.Glaudemans,"Shell-Model Applications in Nuclear Spectroscopy", North Holland,Amesterdam, (1977).
[14]B .A. Brown, R. A. Radhi and B. H. Wildenthal, Phys. Rep., 101, 313, (1983).
[15]R.A.Radhi,A.Al-Rahmani,A.K.Hamoudi and E.A.Salman,Iraq J.Sci,C43,27,(2002).
[16]R.A.Radhi and A.A. Aouda,Proceeding of the first Scientific Conference, 1, 297, (1997).
[17] L. J. Tassie , Austr. J. Phys., 9, 407 , (1956) .
[18]F. I. Shrrad; Ph.D. thesis, College of Science, University of Baghdad, (2007).
[19] T. S. H. Lee and D. Kurath; Phys. Rev., C21, 293, (1980).
[20]B.A.Brown,R.A.Radhi and B.H.Wildenthal; Phys. Rep., 101,313 (1983).
[21] L.J.Tassie ; Austr. J. Phys., 9,407, (1956).
[22] Y. Abgralh and E. Caurier; Phys. Lett., 56B, 229, (1975).
[23] L. S. Cul'karov and R. Kh. Vakil; Nucl. Phys., A43, 515, (1986).
[24]B. E. Norum, M. V. Hynes, H. Miska, W.Bertozzi, J. Kelly, S. Kowalski, F. Rad, C. Sargent, T. Sasanuma and W. Turchinetz; Phys. Rev., C25, 1778, (1982).
[25] V. E. Starodubsky; Nucl. Phys., A219, 525, (1974).
[26] R. Yen, L. S. Cardman, D. Kalinsky, J. R. Legg, C. K. Bockelman; Nucl. Phys., A235, 135, (1974).
[27] J. B. Flanz, R. S. Hicks, R. A. Lindgren, G. A. Peterson, A. Hotta, B. Parker and R. C. York; Phys. Rev. Lett., 41, 1642, (1978).
[28]K. Whitner, C. Williamson and S. Kowalski; Phys. Rev., C22, 374, (1980).
[29]G. C. Li , M. R. Yearian and I. Sick; Phys. Rev., C9, 1861, (1974).
[31] B. H. Wildenthal, B. A. Brown and I. Sick; Phys. Rev., C32, 2185, (1985).
[30]A. Bouchebak; M.Sc. thesis, College of Science, University of Baghdad, (2003).